IJBEM
Vol. 7, No. 2, 2005

An Improved fMRI-EEG Integration Algorithm for Cortical Current Density Estimation by Applying Twomey Regularization

Zhongming Liu, Fedja Kecman, Bin He
Department of Biomedical Engineering, University of Minnesota, MN, USA

Abstract—**We propose to use Twomey regularization to reduce the distortion effects due to fMRI invisible sources in fMRI-constrained cortical current density estimation. Computer simulation was conducted based on a concentric 3-spherical head model. Our proposed method, as well as minimum norm and fMRI-EEG integrated Wiener estimation, were respectively used to image the source distribution over a spherical cortical dipole layer. The performances of these three methods were evaluated both qualitatively and quantitatively. The results show that, at SNR=5, Twomey regularization can reduce the "point spread" from fMRI invisible sources by 34% compared with Wiener estimation, without losing the merit of having much lower point spread from fMRI visible sources than minimum norm solution. The present study suggests that applying Twomey regularization can improve the reliability of multimodal cortical imaging against the misspecifications between EEG and fMRI.**

Keywords—**EEG, fMRI, minimum norm, multimodal neuroimaging, point spread, Twomey regularization, Wiener estimation**

I. Introduction

Tremendous efforts have been made to combine the complementary information from EEG (or MEG) and fMRI for high-resolution spatiotemporal mapping of brain activity. A common strategy for fMRI-EEG integration is to use the results of fMRI analysis as *a priori* knowledge for imaging the continuous distribution of EEG sources over the entire cortical surface, namely fMRI-constrained cortical current density estimation (which we shall call cortical imaging subsequently) [1-3]. Considering the close coupling between local hemodynamic response and neural activity, fMRI "hotspots" (locations with significant hemodynamic change) are preferred in fMRI-constrained cortical imaging, which can be accomplished by encoding the fMRI spatial information into the source covariance matrix and constructing an optimal linear estimator in the form of Wiener filter [1,2]. Previous simulation and experimental studies have demonstrated the importance of using fMRI constraints in enhancing the spatial resolution of EEG- or MEG-based cortical imaging, and applications of this method have already advanced our understanding of the spatiotemporal pattern of brain activation and connectivity underlying perception, motion and cognition [2-5].

However, considering the facts that EEG (or MEG) and fMRI measure physically different aspects of brain activities and that they usually involve a variety of experimental setup and complicated mathematical processing procedures, there are reasons to expect possible misspecifications between multimodal signals, in particular the presence of fMRI invisible (missing) sources (i.e., generators of bioelectromagnetic signals that are not detected by fMRI). Previously, Liu *et al* systematically discussed this issue and concluded that the estimation error as measured by "crosstalk" metric is substantially higher for fMRI invisible sources than for fMRI visible sources [2]. Their studies also suggest applying a 90% partial fMRI constraint without completely excluding the possibility of non-fMRI locations in order to reduce such distorting effects, but fMRI invisible sources are still considerably underestimated or even eliminated especially when the recorded bioelectromagnetic signals are noisy [2,6].

In this paper, we propose to use a modified Tikhonov technique, known as Twomey regularization [7], to correct fMRI-biased source estimates from being distorted by the presence of fMRI invisible sources. Previously, similar concept has been adopted to include the constraint of time progress in electrocardiography inverse problem [8]. In our study, the fMRI-constrained solution obtained through Wiener estimator is only used as the initial estimate of cortical current density, and is subsequently adjusted by fitting it to the EEG data again without fMRI constraints by using Twomey regularization in an attempt to produce a "better" solution. We evaluate the efficacy of this proposed approach in both quality and quantity through computer simulation based on three-spherical head model. All the simulations and discussions are in the context of EEG and fMRI, but the approach is also applicable to integration of MEG and fMRI or PET respectively.

II. Methods

A. Cortical Imaging

Cortical current density estimation [9], known as an EEG inverse problem, is to solve the following linear equation:

$$y = Ax + b \tag{1}$$

where y is the vector of instantaneous EEG recordings, x is the vector of unknown dipole moments, b is the noise vector, and A is the transfer matrix.

If *a priori* information exists about the covariance matrix of source and noise, the optimal linear inverse operator W can be written as Eq(2):

$$W = RA^T\left(ARA^T + C\right)^{-1} \tag{2}$$

where C is the noise covariance matrix and R is the source covariance matrix [1,2].

B. Using fMRI Spatial Information

The integration of EEG and fMRI works under the hypothesis that the regions with great BOLD-fMRI activation have larger possibility of being electrically active over the time period of interest, which suggests that we can use fMRI spatial information to bias the EEG inverse solution to those locations of significant BOLD response. Here, we adopt a 90% partial fMRI weighting as first proposed by Liu *et al* in 1998 [2], simply setting the diagonal elements of R to a nonzero value r only for those dipoles whose locations are visible in fMRI images, and other diagonal elements are set to $0.1r$, leaving all the off-diagonal elements equal to 0. Although it would certainly be preferable to have a more precise and quantitative model to derive dipole source covariance from the fMRI data, unfortunately, at this time the physical and physiological basis that accounts for the correlation between fMRI signal and neural electrical activity is not yet well understood.

Clearly, the source covariance matrix R is a function of r, whose value can be uniquely determined by satisfying Eq(3):

$$tr\left(ARA^T\right) = \gamma^2 tr(C) \tag{3}$$

where $tr(\cdot)$ is the trace of a square matrix and γ is the signal-to-noise ratio (SNR) of the recorded scalp potential. In practice, both γ and C can be estimated from EEG experimental data. Eq(3) requires that the source variance derived from fMRI data must be compatible with the signal variance estimated from EEG measurements.

Once the value of r is chosen, fMRI-constrained current density estimation can be obtained via Eq(4):

$$x^{fMRI} = W^{fMRI} y, \text{ where } W^{fMRI} = RA^T\left(ARA^T + C\right)^{-1} \tag{4}$$

C. Twomey Regularization

Although using fMRI spatial constraints for EEG inverse problem has a sound physiological basis, one might expect that the fMRI hotspots may not cover all the current sources activated at a given instant, giving rise to fMRI invisible sources, which are always underestimated in fMRI-constrained cortical imaging. We attempt to correct such distortion by means of Twomey regularization. Instead of imposing constraints on the magnitude of the solution or on its derivatives, this method minimizes the difference between the desired solution x and a rough estimate x^{fMRI}, as well as the residual error in the least square sense. Hence, the objective function becomes

$$\min_x\left(\left\|Ax - y\right\|^2 + \lambda\left\|x - x^{fMRI}\right\|^2\right) \tag{5}$$

Here, x^{fMRI} is the source vector obtained through the linear inverse operator W^{fMRI} that incorporates fMRI spatial information as described above. We can see that the fMRI spatial constraint has been partially weakened, which yields the robustness of the estimated solution in the face of the possible fMRI misspecifications. If λ, the regularization parameter that balances the two terms in the cost function, is chosen to be a large value the solution is forced to be very close to x^{fMRI}, and it should come as no surprise to expect that the solution is dominated by fMRI spatial constraint and is still sensitive to fMRI invisible sources. On the contrary, if λ is small, the solution tends to shift away from x^{fMRI} in a way to reduce the residual norm, as a result, the source estimation has chance to be corrected against the influence from fMRI-EEG mismatches through better fitting to EEG recordings. And if λ is virtually close to zero, then the solution turns to a purely least square inverse solution, suffering from unstableness and low spatial resolution. Clearly, the trade-off is controlled by λ.

In our study, the objective function was minimized with respect to an inequality constraint which restricts the maximum deflection from the initial estimates.

$$\frac{\left\|x - x^{fMRI}\right\|}{\left\|x^{fMRI}\right\|} \le 0.2 \tag{6}$$

And, Hebden-Newton iteration method was employed to find the optimal value of λ [10].

Given λ is known, the solution to (5) is

$$x_T = \left(A^T A + \lambda I\right)^{-1}\left(A^T y + \lambda x^{fMRI}\right) \tag{7}$$

where $x^{fMRI} = W^{fMRI} y$. In fact, this solution is still a linear inverse solution and the inverse operator is

$$W_T = \left(A^T A + \lambda I\right)^{-1}\left(A^T + \lambda RA^T\left(ARA^T + C\right)^{-1}\right) \tag{8}$$

D. Computer Simulation

In our computer simulation, the performance of the proposed method, abbreviated as *Twomey*, was examined both qualitatively and quantitatively by comparing with minimum norm approach [11] and fMRI-EEG integrated Wiener estimation without Twomey regularization, denoted as *MN* and *Wiener* respectively. The simulation was conducted on an inhomogeneous concentric 3-spherical volume conductor model, which is a reasonable simplification of actual head, with radii of skin, skull and dura mater being 10cm, 9.2cm and 8.7cm respectively. The conductivities of the scalp and the brain were taken as 1.0 and that of the skull as 0.0125. The cortical layer over which 1280 radial dipoles were evenly disposed was also simplified as a spherical surface with radius equal to 0.85.

At a single time point, either 5, 10, 15 or 20 point sources at upper hemisphere of cortical layer were randomly chosen to be activated. To simulate fMRI areas of activation, some of these sources had corresponding fMRI activation with a fixed volumetric extent (1cm radius), while a varying number (1, 2, 3 5, 7…) of other point sources that do not appear in fMRI activation map behave as fMRI invisible sources (or missing sources). EEG measurements were first generated by means of the analytical forward model and 128 electrodes over the upper hemisphere of scalp surface. Subsequently, additive Gaussian white noise was added to the simulated EEG signals with a fixed SNR equal to 5, which is a value consistent with typical EEG experiments.

Due to the linearity of both the forward and inverse problem, a measure of estimation error defined as "point spread" can be calculated for each source location. Mathematically,

$$\rho_i^2 = \frac{\sum_{j \neq i} \left| (WA)_{ji} \right|^2}{\left| (WA)_{ii} \right|^2} \tag{9}$$

where $(WA)_{ji}$ describes the sensitivity of the estimate at a location j to activity at location i. Point spread reflects the spatial blurring of the true activity at any given position. A location with lower point spread has a smaller spatial extent and higher estimation accuracy.

Three source imaging methods (MN, Wiener and Twomey) were used to estimate the current density distribution over the cortical layer. For each different condition defined by the total number of sources and the number of fMRI invisible sources, the random placement of point sources and fMRI areas were repeated for 100 times. The averages of point spread from fMRI invisible sources and from fMRI visible sources were respectively calculated to compare the performance of different inverse methods.

III. Results

Fig. 1 illustrates an example of cortical current density (CCD) results reconstructed respectively through minimum norm approach, Wiener estimation and our proposed method.

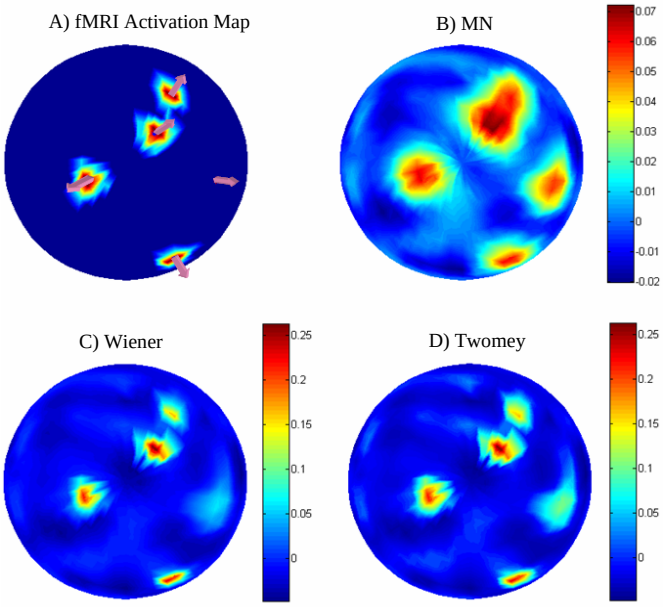

Fig. 1. A) Five radial dipoles (one is fMRI invisible source) and the simulated fMRI activation map. B) Cortical current density (CCD) distribution estimated by minimum norm approach. C) CCD distribution by Wiener estimation. D) CCD distribution after applying Twomey regularization.

Five radial dipoles with unitary strength were randomly sampled from the upper hemisphere of the cortical layer. fMRI activation map was simulated to cover four of the five sources, leaving one to be an fMRI missing source. From Fig. 1.B), MN tends to produce extended areas of current density so that two close dipoles can hardly be differentiated from the reconstructed CCD map. Incorporating fMRI data can greatly enhance the spatial resolution, but the fMRI invisible source is considerably underestimated as shown in Fig. 1.C). After applying Twomey regularization, the reconstructed CCD distribution has equally high resolution for fMRI visible sources as that in Wiener estimation, and it also reveals much stronger activity associated with fMRI invisible sources.

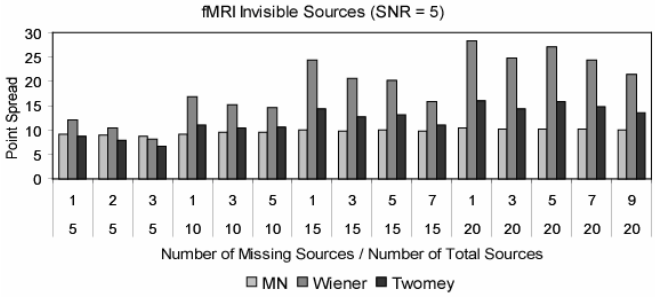

Fig. 2. The average point spread from fMRI invisible sources vs. the number of missing sources and the number of total sources

Fig. 2 shows the average point spread from fMRI invisible sources as a function of the number of missing sources and the number of total sources at SNR equal to 5. In Wiener estimation, the point spread from fMRI invisible sources is substantively higher than that in MN solution. Twomey regularization performed on the basis of the result of Wiener estimation always improves the estimation accuracy for missing sources, especially when the total number of sources is 5 or 10, the point spread from fMRI invisible sources is comparable with that in MN. But when more sources (such as 15 or 20) are activated at the same time, fMRI missing sources are still underestimated compared with MN solution. Averaging among different source configurations, Twomey regularization reduces the point spread from fMRI invisible sources by about 34% relative to Wiener estimation.

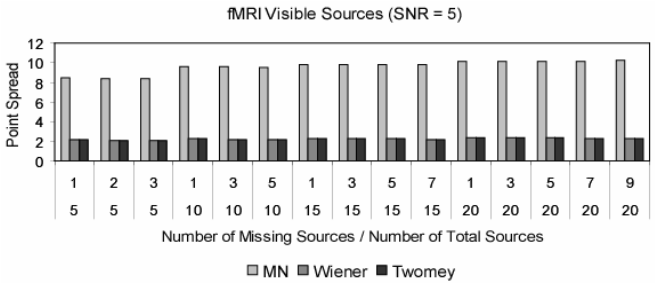

Fig. 3. The average point spread from fMRI visible sources vs. the number of missing sources and the number of total sources

Fig. 3 shows the average point spread from fMRI visible sources. Wiener and Twomey end up with almost identical point spread from fMRI visible sources, which keeps unchanged with respect to different numbers of total sources and missing sources. Clearly, the use of Twomey regularization does not influence the merit of fMRI-EEG integration in providing high-resolution reconstruction of fMRI visible sources.

IV. Discussion

Integration of fMRI and EEG holds the promise to achieve high-resolution spatiotemporal mapping of brain activities. However, the presence of fMRI invisible sources leads to distorted current density reconstruction. In our present study, Twomey regularization was applied to correct such distortion effects. It has been clearly shown in the computer simulation that Twomey regularization, which can be regarded as a post-processing of existing fMRI-EEG integration algorithm, greatly reduces the point spread from fMRI invisible sources at SNR equal to 5 without affecting the estimation accuracy for fMRI visible sources.

Although applying Twomey regularization can alleviate the distortion due to fMRI invisible sources, our simulation results also show that point spread from fMRI invisible sources are still higher than from fMRI visible sources, and even higher than the point spread in minimum norm solution. But considering the dominant advantage of high-resolution estimation of fMRI visible sources, the overall performance of fMRI-EEG integrated cortical current density estimation is superior to that of using EEG data alone, as long as fMRI spatial information, in general, agrees with locations of with neural activity.

The simulation study is based on the 3-spherical head model. Certainly the realistic geometry boundary element model (BEM) or the finite element model (FEM) are more preferable in order to take more practical circumstances into account. However, the three-spherical model is a widely accepted simplification of human head volume conductor. It also allows us to focus on the inherent mathematical aspects of this multimodal neuroimaging problem.

In the present study, EEG measurements were simulated at SNR equal to 5. In practical EEG experiments, SNR depends on the instrumentation and neural tasks specific to a particular study. In our future research, we will conduct the simulation with varying level of SNR.

Acknowledgment

This work was supported in part by NSF-BES-0411898, and NIH EB00178.

References

[1] A. M. Dale and M. I. Sereno, “Improved localization of cortical activity by combining EEG and MEG with MRI cortical surface reconstruction: A linear approach”, J. Cogn. Neurosci., 5, 162-176, 1993.

[2] A. K. Liu, J. W. Belliveau and A. M. Dale, “Spatiotemporal imaging of human brain activity using functional MRI constrained magnetoencephalography data: Monte Carlo simulations”, Proc. Natl. Acad. Sci. USA, 95, 8945-8950, 1998.

[3] F. Babiloni, C. Babiloni, F. Carducci, G. L. Romani, P. M. Rossini, L. M. Angelone and F. Cincotti, “Multimodal integration of high-resolution EEG and functional magnetic resonance imaging data: a simulation study”, NeuroImage, 19, 1-15, 2003.

[4] F. Babiloni, F. Cincotti, C. Babiloni, F. Carducci, D. Mattia, L. Astolfi, A. Basilisco, P.M. Rossini, L. Ding, Y. Ni, J. Cheng, K. Christine, J. Sweeney and B. He, “Estimation of the cortical functional connectivity with the multimodal integration of high-resolution EEG and fMRI data by directed transfer function”, NeuroImage, 24, 118-131, 2005.

[5] A. M. Dale, A. K. Liu, B. R. Fischl, R. L. Buckner, J. W. Belliveau, J. D. Lewine and E. Halgren, “Dynamic statistical parametric mapping: combining fMRI and MEG for high-resolution imaging of cortical activity”, Neuron 26, 55-67, 2000.

[6] A. K. Liu, A. M. Dale and J. W. Belliveau, “Monte Carlo simulation studies of EEG and MEG localization accuracy”, Human Brain Mapping 16, 47-62, 2002.

[7] S. Twomey, “On the numerical solution of Fredholm integral equations of the first kind by the inversion of the linear system produced by qudarature,” J. Assoc. Comput. Mach., 10, 97-101, 1963.

[8] H. S. Oster and Y. Rudy, “The use of temporal information in the regularization of the inverse problem of electrocardiography”, IEEE Trans Biomed. Eng., 39, 65-75, 1992.

[9] B. He, D. Yao and J. Lian, “High-resolution EEG: on the cortical equivalent dipole layer imaging”, Clinic Neurophysiology, 113, 227-235, 2002.

[10] T. F. Chan, J. A. Olkin and D. W. Cooley, “Solving quadratically constrained least squares using black box solvers”, BIT, 32, 481-495, 1992.

[11] M. S. Hamalainen and R. J. Ilmoniemi, “Interpreting measured magnetic fields of the brain: Estimates of current distribution. Helsinki University of Technology, Department of Technical Physics Report, TKK-F-A559.